Published in final edited form as:
*Hepatology*. 2014 June ; 59(6): 2321–2330. doi:10.1002/hep.26925.

# Non-invasive in vivo magnetic resonance measures of glutathione synthesis in human and rat liver as an oxidative stress biomarker

**John T Skamarauskas**[1,2], **Fiona Oakley**[2], **Fiona E Smith**[1,2], **Carlo Bawn**[3], **Michael Dunn**[1,4], **Daniel S Vidler**[1,4], **Matthew Clemence**[5], **Peter G Blain**[1,4], **Roy Taylor**[1,2], **Michael P Gamcsik**[6,#], and **Peter E Thelwall**[1,2,#]

[1]Institute of Cellular Medicine, Newcastle University, Newcastle upon Tyne, UK

[2]Newcastle Magnetic Resonance Centre, Newcastle University, Newcastle upon Tyne, UK

[3]Northern Institute for Cancer Research, Newcastle University, Newcastle upon Tyne, UK

[4]Medical Toxicology Centre, Newcastle University, Newcastle upon Tyne, UK

[5]Philips Healthcare Clinical Science, Guildford, UK

[6]Joint Department of Biomedical Engineering, University of North Carolina, Chapel Hill and North Carolina State University, Raleigh, NC, USA

## Abstract

Oxidative stress plays a central role in the progression of liver disease and in damage to liver via toxic xenobiotics. We have developed methods for non-invasive assessment of hepatic oxidative stress defences by measuring flux through the glutathione synthesis pathway. $^{13}$C-labelled glutathione is endogenously produced and detected by in vivo magnetic resonance following administration of [2-$^{13}$C]-glycine. We report successful first-in-man demonstration of this approach, and preclinical studies demonstrating perturbed glutathione metabolism in models of acute and chronic oxidative stress. Human studies employed oral administration of [2-$^{13}$C]-glycine and $^{13}$C spectroscopy on a 3T clinical MRI scanner, and demonstrated detection and quantification of endogenously produced $^{13}$C-glutathione following labelled glycine ingestion. Plasma analysis demonstrated that glycine $^{13}$C fractional enrichment achieved steady state during the 6h ingestion period. Mean rate of synthesis of hepatic $^{13}$C-labelled glutathione was 0.32 ± 0.18 mmole/kg/h. Preclinical models of acute oxidative stress and non-alcoholic steatohepatitis (NASH) comprised $CCl_4$-treated and high fat, high carbohydrate diet-fed Sprague Dawley rats respectively, using intravenous administration of [2-$^{13}$C]-glycine and observation of $^{13}$C-label metabolism on a 7T preclinical MR system. Preclinical studies demonstrated a 54% elevation of glutathione content and a 31% increase in flux through the glutathione synthesis pathway at 12h after acute insult caused by $CCl_4$ administration, and 23% decrease in glutathione content and evidence of early steatohepatitis in the model of NASH.

Corresponding author: Dr Peter E Thelwall, Newcastle Magnetic Resonance Centre, Campus for Ageing and Vitality, Newcastle University, Newcastle upon Tyne, NE4 5PL, UK, Phone: +44 191 248 1250, pete.thelwall@ncl.ac.uk.
[#]Joint senior authors

**Conflict of interest**: MC is a full time employee of Philips Healthcare.

**Conclusion—**Our data demonstrate in vivo $^{13}$C-labelling and detection of glutathione as a biomarker of tissue oxidative stress defences, detecting chronic and acute oxidative stress insults. The methods are applicable to clinical research studies of hepatic oxidative stress in disease states over time as well as to monitoring the effects of therapeutic interventions.

### Keywords

$^{13}$C spectroscopy; dynamic magnetic resonance; metabolism; glutathione synthetase; serine hydroxymethyltransferase

## Introduction

Tissue oxidative stress results from an excess of reactive oxygen species (ROS), resulting in an inability of cells to maintain a reduced intracellular environment. Hepatic oxidative stress is central to the processes involved in the progression of liver disease (1-3), and the cell has evolved multiple mechanisms to protect itself from oxidative stress: DNA repair, enzymes that catalyse the deactivation of free radicals, and antioxidants of endogenous or dietary origin. ROS and pro-oxidants can arise within a tissue from multiple endogenous and exogenous sources, such as by-products of oxidative phosphorylation, components of an immune response, from xenobiotics, or the generation of reactive intermediates as a result of catabolic processes (1). The principal hepatic intracellular antioxidant is glutathione, a tripeptide of glycine, cysteine and glutamate that is synthesised in two steps from its constituent amino acids by γ-glutamylcysteine synthetase and glutathione synthetase (3,4). Glutathione has a central role in protecting the cell against ROS and in detoxifying xenobiotics, homeostatic processes strive to maintain hepatic glutathione content and maintain a reduced intracellular environment.

A wealth of preclinical studies have investigated hepatic responses to oxidative stress via change in glutathione content or glutathione synthesis enzyme activities (5). In addition, blood-based indirect markers of oxidative stress have been identified, typically comprising byproducts of oxidative stress (eg. lipid peroxidation byproducts) (6-8), along with measurements in liver biopsy samples of glutathione content, enzyme activities and expression of genes related to oxidative stress defence (eg. (9,10)). However, direct tissue sampling is invasive and carries an associated risk to the patient, and blood biomarkers report on downstream effects of oxidative stress rather than providing direct measures of cellular redox defences.

We have developed methods to monitor liver glutathione metabolism *in vivo*, providing a non-invasive biomarker that reports directly on hepatic oxidative stress defences. In our previous studies we have demonstrated that administration of $^{13}$C-labelled glycine results in the metabolic production of γ-glutamylcysteinyl-[2-$^{13}$C]-glycine (referred to hereafter as $^{13}$C-glutathione), and that in vivo monitoring of this $^{13}$C-labelling process can be performed by MRI (11-13). In this study we translate this approach to human liver for clinical research studies, and show alterations in glutathione metabolism in response to chronic and acute oxidative stress insults in preclinical models.

Our preclinical studies employ two models of hepatic oxidative stress: an acute insult resultant from carbon tetrachloride (CCl4) administration, and chronic oxidative stress generated from a high fat, high carbohydrate diet model of steatohepatitis. CCl4 administration has been widely employed to generate hepatic oxidative stress and to study hepatotoxicity, fibrosis, hepatocellular death and carcinogenicity (14), and allows us to gauge change in hepatic glutathione turnover after acute oxidative stress insult. Our diet-induced steatohepatitis model was based on that described by Kohli et al. (15) as a model of chronic oxidative stress, which exhibited a non-alcoholic steatohepatitis (NASH) phenotype. Our model comprised an 8 week diet duration, with the aims of producing early non-alcoholic steatohepatitis and testing whether our MR approach can detect changes in tissue oxidative stress defences at this stage of NASH progression.

The purpose of our study was to translate the glutathione $^{13}$C-labelling approach to human studies, to perform preclinical studies of controlled acute and chronic oxidative stress insult, and thus demonstrate utility of glutathione metabolism monitoring as a biomarker of perturbed hepatic redox defences suitable for application to clinical research studies.

## Materials and Methods

### Preclinical study: Experimental design

Preclinical studies were performed under a project licence granted by the Home Office in accordance with the Animals (Scientific Procedures) Act 1986. [2-$^{13}$C]-Glycine was purchased from Cambridge Isotope Laboratories Inc (Andover, MA, USA) and from Sigma-Aldrich (Gillingham, UK). Three groups of male Sprague Dawley rats (Charles River, Margate, UK) comprised control, $CCl_4$-induced acute oxidative stress, and rats fed a high fat and high-carbohydrate (HFHC) diet to induce steatohepatitis (n=7 per group). $CCl_4$-treated rats received a 1:1 mixture of $CCl_4$ and refined olive oil (0.1 mL per 100g body weight, i/p injection) at 12h before the MR study. The HFHC diet comprised ad libitum feed containing 60% kcal from fat (TestDiet 58R2; IPS Ltd, London, UK) and drinking water supplemented with 55 mmol/l sucrose and 128 mmol/l fructose for 8 weeks prior to MR experiments.

### Preclinical study: Magnetic resonance spectroscopy

Figure 1A shows the relative timing of [2-$^{13}$C]-glycine infusion and MR data acquisitions. MR studies were started at the same time each day (10am) to avoid the influence of diurnal variation in glutathione synthesis rate on study data (16). Rats were anesthetised with i/p-administered solution of fentanyl (0.79 mg/mL), fluanisone (2.5 mg/mL) and midazolam (1.25 mg/mL) in water at a dose of 0.2 mL/kg, and maintenance doses were administered as required via an MR-compatible i/p cannula. Intravenous administration of [2-$^{13}$C]-glycine in water (1M, pH 7.4) was via a tail vein catheter. Respiratory and body temperature monitoring was performed during MR experiments. $^{1}$H-decoupled $^{13}$C spectra were acquired on a Varian 7T magnet and spectrometer (DirectDrive system, Varian Inc, Palo Alto, CA) using a custom $^{13}$C/$^{1}$H coil (15mm diameter $^{13}$C coil, Figure 2A). Positioning of the coil relative to the liver is shown in Figures 2C and E. $^{13}$C spectra were acquired every 10 minutes for the experiment duration (tip angle = 90°, TR = 1.5s, sw = 10kHz, 400 averages). [2-$^{13}$C]-glycine delivery commenced after acquisition of baseline MR data at a

loading dose of 4 mmoles/kg/h for 90 minutes, then at a maintenance dose of 1 mmole/kg/h for 5 hours. Details of preparation of liver tissue perchloric acid extracts, of $^{1}$H NMR and mass spectrometry analysis of liver and plasma samples, of preparation of histological section, and of MR data analysis and quantitation are provided in the Supplementary Materials. Statistical significance of differences in concentrations and rates between experimental groups was determined using one-way ANOVA with Tukey multiple comparisons (Minitab 16, Minitab Inc, State College, PA, USA).

### Human study: Subjects and experimental design

Ethical permission for the study was obtained from the Newcastle and North Tyneside 1 Research Ethics Committee. Healthy male volunteers (n=3) were recruited from the staff of Newcastle University and informed consent was obtained. Subjects abstained from alcohol for 3 days prior to the study and fasted from 11.30pm on the evening before the study (water *ad libitum*). The study commenced at 8.30am the following day with acquisition of baseline liver $^{13}$C spectra. Figure 1B shows timing of [2-$^{13}$C]-glycine administration, blood sampling and MR examinations. [2-$^{13}$C]-glycine was purchased from Cambridge Isotope Laboratories (Andover, MA, USA), administration consisted of twelve doses of 3g of [2-$^{13}$C]-glycine dissolved in 50 mL of water, ingested orally at 30 minute intervals over a 6h period. Glycine administration commenced immediately after acquisition of baseline liver MR spectra, and MR data acquisition and was repeated at 2, 4, 6 and 8 hours. Plasma samples were stored at -40 °C prior to analysis of total and [2-$^{13}$C]-labelled glycine content by $^{1}$H NMR as described in the Supplementary Materials. Volunteers ate a standardised lunch (comprising a sandwich, an apple and water) at 165 min after commencing glycine ingestion. The experimental protocol was designed to replicate the preclinical studies as closely as possible, though [2-$^{13}$C]-glycine administration was oral instead of by intravenous infusion. This provided delivery of label to the liver via the portal vein, and represented a pragmatic approach for ethical review committee consideration of this first-in-man healthy volunteer study.

### Human study: $^{13}$C magnetic resonance spectroscopy

Magnetic resonance imaging and spectroscopy measurements were made using a Philips Achieva 3T whole body scanner (Philips Medical Systems, Best, The Netherlands) and an in-house $^{13}$C/$^{1}$H surface coil (12 cm diameter $^{13}$C coil, Figure 2B) positioned over the liver. A representative image showing positioning of the $^{13}$C coil is shown in Figures 2D and F. $^{13}$C spectra were acquired using a pulse-acquire sequence with $^{1}$H WALTZ decoupling (TR = 1.5s, nominal tip angle = 90°, 1024 datapoints, 8 kHz spectral width, 15 minute scan duration). Concentrations of $^{13}$C-labelled metabolites were determined from spectra as described in the Supplementary Materials.

## Results

### Preclinical studies: perturbed glutathione turnover is observed following acute and chronic oxidative stress insults

Table 1 shows rat morphometric measurements, plasma biochemical analysis, and hepatic $F_2$-isoprostane content analysis. $CCl_4$ treatment resulted in a significant elevation of plasma

AST and ALT relative to the control group, indicative of acute liver damage ($p < 0.05$). Quantitation of hepatic $F_2$-isoprostanes as a biomarker of lipid peroxidation demonstrated significant elevation in both the $CCl_4$-treated and HFHC diet groups compared to control, indicating oxidative stress insults.

Figure 3 shows $^{13}C$ spectra and calculated metabolite concentrations from the preclinical experimental studies. Figure 3A shows a representative rat hepatic $^{13}C$ spectrum acquired at 6h after commencement of [2-$^{13}C$]-glycine administration. Resonances from infused [2-$^{13}C$]-glycine and from endogenously produced $^{13}C$-labelled glutathione are clearly observed at 42.4 ppm and 44.2 ppm respectively, adjacent to natural abundance $^{13}C$ resonances from lipids in the 35 - 14 ppm region. The highlighted region of this spectrum (50-40 ppm) is shown in Figure 3B, comprising representative spectra from the three experimental groups acquired at the 5h experimental timepoint, showing the [2-$^{13}C$]-glycine and $^{13}C$-glutathione resonances. Differences in both $^{13}C$-glutathione and [2-$^{13}C$]-glycine concentration are apparent between the groups, reflecting insult-induced differences in both glutathione and glycine metabolism.

Dynamic measurements of hepatic $^{13}C$-labelled glutathione content were made over the mental timecouse, and are shown for the three groups in Figure 3C. A marked and statistically significant ($p < 0.05$) elevation of $^{13}C$-glutathione content is observed in the $CCl_4$-treated group compared to the other groups ($1.71 \pm 0.39$ compared to $1.11 \pm 0.19$ mmol/l for the control group at 5h), consistent with hepatic response to the acute oxidative stress insult. Conversely, rats in HFHC diet group showed slightly lower $^{13}C$-glutathione than the control group ($0.86 \pm 0.18$ mmol/l) indicating a lower glutathione turnover, though this difference was not statistically significant. However, total glutathione content was significantly lower than control in the HFHC group, and significantly elevated in the $CCl_4$-treated group ($p < 0.05$, Figure 3D). The data demonstrate the model of early NASH exhibiting compromised oxidative stress defences (with consequent potential for cellular damage), in contrast to the acute $CCl_4$ insult resulting in a strong upregulation of glutathione production. The rate of $^{13}C$-label incorporation into the hepatic glutathione pool also reflects these group differences, showing a higher rate for $CCl_4$-treated rats than for the other groups, with an initial rate (measured between t=30 and 90 min) of $0.76 \pm 0.14$ mmoles/kg/h compared to $0.58 \pm 0.09$ and $0.48 \pm 0.07$ mmoles/kg/h for control and HFHC groups respectively ($p < 0.05$).

Hepatic [2-$^{13}C$]-glycine content over the experiment duration is shown in Figure 3E, charting the effect of label infusion. All three groups show a similar pattern: a rapid rise during the initial 90 minutes high infusion rate, followed by maintenance of [2-$^{13}$-glycine concentration at approximately 4 mmol/l. The infusion scheme was chosen to rapidly maximise and then maintain hepatic glycine $^{13}C$ fractional enrichment. Minor differences between groups are observed after ~3h, the $CCl_4$-treated group shows a downward trend in [2-$^{13}C$]-glycine concentration from 2-6 h, whereas the HFHC-diet group shows a slight upward trend. $^1H$ MRS measurements of glycine $^{13}C$ fractional enrichment in extract samples were $57 \pm 4\%$, $59 \pm 5\%$ and $69 \pm 2\%$ in the control, $CCl_4$-treated and HFHC groups respectively at the end of the infusion period, with the HFHC group measurement significantly different from control ($p < 0.05$). We attribute these differences to variations in

flux through glycine metabolism pathways: in addition to alterations in flux of $^{13}C$ label to glutathione we also observed differences in flux through serine hydroxymethyltransferase to $^{13}C$-labelled serine. Our preclinical study protocol did not permit serial sampling of plasma to measure glycine $^{13}C$ fractional enrichment, but previous studies by Macdonald et al (11) and by Fern and Garlick (17) demonstrate that a similar infusion of labelled glycine results in steady state being achieved rapidly and within 2h, and our human studies demonstrated glycine fractional enrichment reaching steady state within 2h (*vide infra*).

Figure 3F shows hepatic [2-$^{13}C$]-serine content, with the $CCl_4$-treated group showing an elevated concentration of labelled serine compared to the other groups. This difference was statistically significantly compared to control at the 1.5h timepoint, and compared to the HFHC group at the 1.5, 3 and 5h timepoints ($p < 0.05$).

Figure 4 shows histological sections from the three groups stained with Haematoxylin and Eosin, α-SMA for myofibroblast visualisation, and Sirius red as a marker of collagen deposition. Liver histology was normal for the control group, whereas the $CCl_4$-treatment group shows hallmarks of acute oxidative stress (ballooned and swollen dead/dying hepatocytes and the emergence of hepatic myofibroblasts). The HFHC group shows early steatohepatitis, including fat deposition, activation of hepatic myofibroblasts, and collagen deposition.

Mass spectrometry analysis of glutathione tissue extracts identified a fraction of the glutathione containing two $^{13}C$ nuclei per molecule. We have observed similar labelling in our previous studies of tumour oxidative stress defences (13), and attribute this to synthesis of $^{13}C$-label in the cysteinyl residue of glutathione. Incorporation of $^{13}C$ label from [2-$^{13}C$]-glycine into cysteine occurs via the trans-sulfuration pathway (18), with labelled serine as an intermediate. The percentage of doubly $^{13}C$-labelled glutathione was 2.9 ± 0.8, 4.1 ± 1.7 and 6.2 ± 1.6% for the control, $CCl_4$-treated and HFHC diet groups respectively. The HFHC group shows a significantly higher degree of double $^{13}C$-labelling than the other groups ($p < 0.05$), indicating higher production of cysteine via the trans-sulfuration pathway. This may originate from dietary differences between the groups, with lower protein intake in the HFHC group resulting in upregulation of trans-sulfuration to supply cysteine (18).

## Human studies: Hepatic $^{13}C$-labelled glutathione can be detected and quantified following ingestion of [2-$^{13}C$]-glycine

Study participants were male, had an average age of 32 ± 4 years and a body weight of 75 ± 3 kg. Standard plasma clinical biochemistry assays reported normal results for all participants. Hepatic $^{13}C$ spectra showed well-resolved resonances from [2-$^{13}C$]-glycine and $^{13}C$-glutathione, allowing quantification of $^{13}C$-label incorporation into glutathione over the experimental timecourse. Figure 5A shows spectra from a participant acquired before and at 6h after commencement of [2-$^{13}C$]-glycine ingestion. The spectrum is similar in appearance to the preclinical studies (reflecting the similarities in experimental approach), though a broader region of the spectrum is observed due to the lower magnetic field strength of the human whole body scanner (3T rather than 7T). Figure 5B shows the 65-35 ppm spectra region from the same subject at the five experimental timepoints, showing the administered [2-$^{13}C$]-glycine and its subsequent metabolism. Signal from labelled glycine is

observed at the first measurement after ingestion (2h), and its magnitude is maximal at the end of the 6h ingestion period. Incorporation of the $^{13}$C label into the 2-carbon of the glycinyl residue of glutathione (44.2 ppm) and into other metabolites of glycine was also observed from the 2h timepoint onwards. These other metabolites included [2-$^{13}$C]- and [3-$^{13}$C]-serine at 57.4 and 61.3 ppm respectively, choline and/or creatine at 54.8 ppm, and a resonance at 45.8 ppm that may originate from intermediates in the formation of creatine and choline, guanidoacetate or dimethylglycine. Figure 5C-E show the mean concentrations of $^{13}$C-labelled glycine, glutathione, and serine in human liver over the experimental timecourse. The data demonstrate the rapid turnover of glutathione, and rapid flux of glycine to serine, with appearance of both by the 2h timepoint and appreciable drop in concentration 2h after ingestion of [2-$^{13}$C]-glycine had ceased (8h timepoint).

Figure 6 shows the $^{13}$C fractional enrichment and total concentration of plasma glycine in the human studies. $^{13}$C fractional enrichment was constant at 64.0 ± 6.6 % during the glycine ingestion period. This indicates that steady state labelling was achieved, and thus the incorporation of $^{13}$C label into glutathione reflects the flux through the glutathione pathway rather than the changing $^{13}$C-labelling of the glycine pool. The concentration of plasma glycine peaked at 1.8 ± 0.7 mM at the 6h timepoint.

The initial rate of incorporation of $^{13}$C label into glutathione, measured between the 0 and 2h timepoints, was 0.32 ± 0.18 mmol/kg/h. Highest concentrations of $^{13}$C-labelled metabolites were observed at the end of the [2-$^{13}$C]-glycine administration period, peak hepatic [2-$^{13}$C]-glycine concentration was 2.3±1.5 mmol/l, whereas $^{13}$C-glutathione and [2-$^{13}$C]-serine concentrations were 1.0±0.4 mmol/l and 1.3±0.6 mmol/l respectively.

## Discussion

### $^{13}$C MR Spectroscopy provides a repeatable non-invasive in vivo measure of glutathione synthetic rate

Our data demonstrate successful quantitation of endogenously produced $^{13}$C-labelled glutathione in human liver and perturbed glutathione concentration and turnover rate in rodent models of acute and chronic hepatic oxidative stress. The non-invasive nature of magnetic resonance provides a safe and repeatable tool applicable to hepatic clinical research, avoiding the need for biopsy sampling. A broad range of biomarkers have been employed in numerous preclinical and clinical studies to report on oxidative stress. Those centred on glutathione include glutathione content, the activities of enzymes involved in glutathione synthesis and adduct formation, and the concentrations of other cellular antioxidants and activities of their associated enzymes (5,19-22). However, glutathione concentration and enzyme activity measurements do not necessarily reflect flux through glutathione synthesis and utilisation pathways, and small differences in the balance between glutathione synthesis and utilisation may underlie the literature conflict on, for example, whether $CCl_4$ causes an acute increase or decrease in glutathione content (4,22,23). In this regard our dynamic $^{13}$C-labelling approach may afford a useful and robust metric for assessment of cellular response to hepatic oxidative stress by reporting on flux rather than steady state concentrations of glutathione.

Although our method does not distinguish between reduced and oxidised glutathione (as the chemical shift of the $^{13}C$ label is unaffected by glutathione redox state), our data demonstrate that changes in hepatic glutathione turnover and content provide a sensitive redox defence biomarker. Future work using a labelling scheme of a $^{13}C$ nucleus close to the glutathione thiol group may allow the reduced and oxidised forms of glutathione to be distinguished. The present studies were conducted using [2-$^{13}C$]-glycine as this compound is well tolerated at elevated concentrations, as it has a $^{13}C$ resonance distinct from other resonances in the spectrum, and unlike cysteine is not rate-limiting for glutathione synthesis (5). A method to measure glutathione synthesis via incorporation of $^{3}H$-labelled cysteine into glutathione has been previously employed in clinical research studies (24,25). Our method has some similarities in approach but has the advantage of providing a direct, dynamic and radiolabel-free tissue glutathione content measurement.

Performance of $^{13}C$ MR spectroscopy is not a standard capability for the majority of MRI scanners in current use. However, all major MRI scanner manufacturers have 3T scanner products capable of $^{13}C$ spectroscopy and appropriate RF coils are commercially available. We consider our technique most suited to clinical research studies at present (where human application of $^{13}C$ MR spectroscopy has played an important role to date), and precedents exist for translation of $^{13}C$ MR to use in clinical diagnosis (26). The cost of [2-$^{13}C$]-glycine for our studies was twice the cost of per-volunteer access to the MR scanner, and thus not prohibitive for clinical research. Furthermore, refinement of the experimental protocol to use lower quantities of $^{13}C$ label (by lower total dose or shorter administration period) may be possible given the achieved spectral quality. The higher variance in label incorporation into glutathione in humans compared to the preclinical studies may reflect greater inter-individual biological variation, and/or differences in methodology (oral vs. intravenous label administration). However, the variance in human $^{13}C$-glutathione synthesis rates was similar to that observed in other studies with similar methodological approaches, such as measurement of human hepatic glycogen synthesis rate (eg. (27)).

Brain glutathione content measurements have been made by $^{1}H$ MR spectroscopy (28,29). This approach is well suited to normal and neoplastic brain tissue, but is unable to report on glutathione flux and performs less well in other tissues due to shorter $T_2$ relaxation times and significant contributions to the $^{1}H$ spectrum from lipids. A recent and novel MR approach has employed dynamic nuclear polarisation (DNP) methods to measure the equilibrium flux between $^{13}C$-labelled ascorbic and dehydroascorbic acid as an in vivo probe of tissue redox state (30,31). DNP provides a method to greatly increase the MR signal from an exogenously administered compound such as $^{13}C$-labelled ascorbate, and permits measurement of enzyme flux over a short (tens of seconds) timescale. However, the approach requires administration of considerable quantities of $^{13}C$-labelled tracer, which may have the potential to alter redox balance. In our studies we employed conventional $^{13}C$ spectroscopy, permitting measurements of glutathione metabolism over a 6.5h time period and using a tracer molecule that can be administered without altering the rate of glutathione synthesis (5).

### Hepatic oxidative stress results in significant perturbation of glutathione turnover, measurable by non-invasive $^{13}$C MR spectroscopy

Our human studies represent translation of a novel methodology with potential for direct quantitation of glutathione content and synthesis rate in man as a biomarker. Studies of biopsy samples have demonstrated decreased glutathione content in NAFLD and NASH patients ((10,32), a finding echoed by our preclinical data), and have investigated the impact of therapeutic regimes (eg. (33)). Our non-invasive approach provides a direct measurement from liver tissue (as compared to indirect blood biomarkers) without the need for invasive biopsy. The preclinical models of acute and chronic oxidative stress exhibited insult impact in tissue histology, plasma biomarker assay results, mass spectrometry analysis of isoprostane content, and in C MR measures of glycine and glutathione metabolism. A major acute oxidative stress insult with adaptive changes in glutathione concentration and turnover was produced by $CCl_4$ administration, whereas a mild chronic insult with evidence of compromised oxidative stress defences and early histological signs of steatohepatitis was produced in the HFHC dietary model. $F_2$-isoprostanes provide a biomarker of lipid peroxidation and thus tissue oxidative stress (34), elevated concentrations have been reported in patients with NAFLD (35) and in rat models of hepatic fibrosis (36). The elevated levels observed in the $CCl_4$-treated and HFHC diet groups provides confirmation that the experimental insults resulted in hepatic oxidative stress.

The $CCl_4$-treated group exhibited an approximately 50% increase in glutathione concentration and $^{13}$C label incorporation rate, reflecting a cellular response of increased of glutathione synthesis and utilisation. We chose to perform our MR studies at 12h after $CCl_4$ administration to coincide with a large impact on tissue oxidative stress and cellular response to the insult (37), and the significant effect of the insult was also observed in the biochemical and histological measurements.

Previous studies using the HFHC dietary model of NASH have demonstrated florid NASH developing over a 16 week period (15). Our studies employed an 8 week HFHC dietary feeding period, and isoprostane analysis and histology confirmed hepatic oxidative stress and the appearance of a NASH phenotype in our experimental group at the end of this period. Our studies were limited to an eight week duration in part by the animal size constraints imposed by our preclinical MR scanner. Decreased hepatic glutathione content was observed in this group, along with elevated flux through the trans-sulfuration pathway and decreased serine hydroxymethyltransferase flux. Future studies to investigate the progression of the HFHC dietary model to florid NASH beyond the stage employed in our studies would provide information on the changing hepatic oxidative stress environment and resultant cellular adaptations.

In summary, our data demonstrate in vivo $^{13}$C-labelling and non-invasive detection of glutathione following ingestion (human) or intravenous infusion (rat) of [2-$^{13}$C]-glycine. Clinical research applications for this novel methodology include directly quantifying the impact of glutathione-depleting xenobiotics such as acetaminophen, of drugs that elevate glutathione synthesis rate via supply of rate-limiting substrate such as N-acetyl cysteine or S-adenosyl methionine, and of disease processes involving oxidative stress and perturbed hepatic oxidative stress defences, such as steatohepatitis.

## Supplementary Material

Refer to Web version on PubMed Central for supplementary material.

## Acknowledgments

The study participants are gratefully acknowledged for their contribution to this work. Thanks to Dr Hollingsworth for assistance with $B_0$ mapping methodology, to Dr Anstee for advice on preclinical dietary models of liver disease, and to Louise Morris, Carol Smith and Tim Hodgson for assistance with human data acquisition. Thanks to Margaret Knight and Clair Roper for help with extract sample preparation.

**Financial support**: This work was supported by grant G0801239 from the Medical Research Council, UK (P.E.T.) and by grant R01CA114365 from the National Institutes of Health (M.P.G.).

## References

1. Cesaratto L, Vascotto C, Calligaris S, Tell G. The importance of redox state in liver damage. Ann Hepatol. 2004; 3:86–92. [PubMed: 15505592]
2. Loguercio C, Federico A. Oxidative stress in viral and alcoholic hepatitis. Free Radic Biol Med. 2003; 34:1–10. [PubMed: 12498974]
3. Poli G. Pathogenesis of liver fibrosis: role of oxidative stress. Mol Aspects Med. 2000; 21:49–98. [PubMed: 10978499]
4. Lu SC. Regulation of hepatic glutathione synthesis: current concepts and controversies. FASEB J. 1999; 13:1169–1183. [PubMed: 10385608]
5. Hayes JD, McLellan LI. Glutathione and glutathione-dependent enzymes represent a co-ordinately regulated defence against oxidative stress. Free Radic Res. 1999; 31:273–300. [PubMed: 10517533]
6. Tuma DJ. Role of malondialdehyde-acetaldehyde adducts in liver injury. Free Radic Biol Med. 2002; 32:303–308. [PubMed: 11841919]
7. Sumida Y, Nakashima T, Yoh T, Furutani M, Hirohama A, Kakisaka Y, et al. Serum thioredoxin levels as a predictor of steatohepatitis in patients with nonalcoholic fatty liver disease. J Hepatol. 2003; 38:32–38. [PubMed: 12480557]
8. Iuliano L, Micheletta F, Natoli S, Ginanni Corradini S, Iappelli M, Elisei W, et al. Measurement of oxysterols and alpha-tocopherol in plasma and tissue samples as indices of oxidant stress status. Anal Biochem. 2003; 312:217–223. [PubMed: 12531208]
9. Hardwick RN, Fisher CD, Canet MJ, Lake AD, Cherrington NJ. Diversity in antioxidant response enzymes in progressive stages of human nonalcoholic fatty liver disease. Drug Metab Dispos. 2010; 38:2293–2301. [PubMed: 20805291]
10. Malaguarnera L, Madeddu R, Palio E, Arena N, Malaguarnera M. Heme oxygenase-1 levels and oxidative stress-related parameters in non-alcoholic fatty liver disease patients. J Hepatol. 2005; 42:585–591. [PubMed: 15763346]
11. Macdonald JM, Schmidlin O, James TL. In vivo monitoring of hepatic glutathione in anesthetized rats by 13C NMR. Magn Reson Med. 2002; 48:430–439. [PubMed: 12210907]
12. Thelwall PE, Yemin AY, Gillian TL, Simpson NE, Kasibhatla MS, Rabbani ZN, et al. Noninvasive in vivo detection of glutathione metabolism in tumors. Cancer Res. 2005; 65:10149–10153. [PubMed: 16287997]
13. Thelwall PE, Simpson NE, Rabbani ZN, Clark MD, Pourdeyhimi R, Macdonald JM, et al. In vivo MR studies of glycine and glutathione metabolism in a rat mammary tumor. NMR Biomed. 2011
14. Weber LWD, Boll M, Stampfl A. Hepatotoxicity and mechanism of action of haloalkanes: carbon tetrachloride as a toxicological model. Crit Rev Toxicol. 2003; 33:105–136. [PubMed: 12708612]
15. Kohli R, Kirby M, Xanthakos SA, Softic S, Feldstein AE, Saxena V, et al. High-fructose, medium chain trans fat diet induces liver fibrosis and elevates plasma coenzyme Q9 in a novel murine model of obesity and nonalcoholic steatohepatitis. Hepatology. 2010; 52:934–944. [PubMed: 20607689]

16. Xu YQ, Zhang D, Jin T, Cai DJ, Wu Q, Lu Y, et al. Diurnal variation of hepatic antioxidant gene expression in mice. PLoS ONE. 2012; 7:e44237. [PubMed: 22952936]
17. Fern EB, Garlick PJ. The specific radioactivity of the precursor pool for estimates of the rate of protein synthesis. Biochem J. 1973; 134:1127–1130. [PubMed: 4762757]
18. Finkelstein JD. Methionine metabolism in mammals. J Nutr Biochem. 1990; 1:228–237. [PubMed: 15539209]
19. Pastore A, Federici G, Bertini E, Piemonte F. Analysis of glutathione: implication in redox and detoxification. Clin Chim Acta. 2003; 333:19–39. [PubMed: 12809732]
20. Wang HM, Bodenstein M, Markstaller K. Overview of the pathology of three widely used animal models of acute lung injury. Eur Surg Res. 2008; 40:305–316. [PubMed: 18349543]
21. Cabré M, Camps J, Paternáin JL, Ferré N, Joven J. Time-course of changes in hepatic lipid peroxidation and glutathione metabolism in rats with carbon tetrachloride-induced cirrhosis. Clin Exp Pharmacol Physiol. 2000; 27:694–699. [PubMed: 10972535]
22. Nishida K, Ohta Y, Ishiguro I. Gamma-glutamylcysteinylethyl ester attenuates progression of carbon tetrachloride-induced acute liver injury in mice. Toxicology. 1998; 126:55–63. [PubMed: 9585092]
23. Nakagawa K. Carbon tetrachloride-induced alterations in hepatic glutathione and ascorbic acid contents in mice fed a diet containing ascorbate esters. Arch Toxicol. 1993; 67:686–690. [PubMed: 8135659]
24. Lauterburg BH, Davies S, Mitchell JR. Ethanol suppresses hepatic glutathione synthesis in rats in vivo. J Pharmacol Exp Ther. 1984; 230:7–11. [PubMed: 6747833]
25. Lauterburg BH, Mitchell JR. Therapeutic doses of acetaminophen stimulate the turnover of cysteine and glutathione in man. J Hepatol. 1987; 4:206–211. [PubMed: 3584929]
26. Ross B, Lin A, Harris K, Bhattacharya P, Schweinsburg B. Clinical experience with 13C MRS in vivo. NMR Biomed. 2003; 16:358–369. [PubMed: 14679500]
27. Krssak M, Brehm A, Bernroider E, Anderwald C, Nowotny P, Dalla Man C, et al. Alterations in postprandial hepatic glycogen metabolism in type 2 diabetes. Diabetes. 2004; 53:3048–3056. [PubMed: 15561933]
28. Opstad KS, Provencher SW, Bell BA, Griffiths JR, Howe FA. Detection of elevated glutathione in meningiomas by quantitative in vivo 1H MRS. Magn Reson Med. 2003; 49:632–637. [PubMed: 12652533]
29. Terpstra M, Marjanska M, Henry PG, Tkác I, Gruetter R. Detection of an antioxidant profile in the human brain in vivo via double editing with MEGA-PRESS. Magn Reson Med. 2006; 56:1192–1199. [PubMed: 17089366]
30. Bohndiek SE, Kettunen MI, Hu DE, Kennedy BWC, Boren J, Gallagher FA, et al. Hyperpolarized [1- 13C]-Ascorbic and Dehydroascorbic Acid: Vitamin C as a Probe for Imaging Redox Status in Vivo. J Am Chem Soc. 2011; 133:11795–11801. [PubMed: 21692446]
31. Keshari KR, Kurhanewicz J, Bok R, Larson PEZ, Vigneron DB, Wilson DM. Hyperpolarized 13C dehydroascorbate as an endogenous redox sensor for in vivo metabolic imaging. Proceedings of the National Academy of Sciences. 2011; 108:18606–18611.
32. Videla LA, Rodrigo R, Orellana M, Fernandez V, Tapia G, Quiñones L, et al. Oxidative stress-related parameters in the liver of non-alcoholic fatty liver disease patients. Clin Sci. 2004; 106:261–268. [PubMed: 14556645]
33. Vendemiale G, Altomare E, Trizio T, Le Grazie C, Di Padova C, Salerno MT, et al. Effects of oral S-adenosyl-L-methionine on hepatic glutathione in patients with liver disease. Scand J Gastroenterol. 1989; 24:407–415. [PubMed: 2781235]
34. Roberts LJ, Morrow JD. Measurement of F(2)-isoprostanes as an index of oxidative stress in vivo. Free Radic Biol Med. 2000; 28:505–513. [PubMed: 10719231]
35. Konishi M, Iwasa M, Araki J, Kobayashi Y, Katsuki A, Sumida Y, et al. Increased lipid peroxidation in patients with non-alcoholic fatty liver disease and chronic hepatitis C as measured by the plasma level of 8-isoprostane. J Gastroenterol Hepatol. 2006; 21:1821–1825. [PubMed: 17074020]

36. Comporti M, Arezzini B, Signorini C, Sgherri C, Monaco B, Gardi C. F2-isoprostanes stimulate collagen synthesis in activated hepatic stellate cells: a link with liver fibrosis? Lab Invest. 2005; 85:1381–1391. [PubMed: 16127424]

37. Wang PY, Kaneko T, Tsukada H, Nakano M, Nakajima T, Sato A. Time courses of hepatic injuries induced by chloroform and by carbon tetrachloride: comparison of biochemical and histopathological changes. Arch Toxicol. 1997; 71:638–645. [PubMed: 9332701]

## Abbreviations

| | |
|---|---|
| **$CCl_4$** | Carbon tetrachloride |
| **DNP** | Dynamic nuclear polarisation |
| **$^{13}$C-Glutathione** | γ-glutamylcysteinyl-[2-$^{13}$C]-glycine |
| **H&E** | Haematoxylin and eosin |
| **HFHC** | High fat, high carbohydrate diet |
| **MRI** | Magnetic Resonance Imaging |
| **MRS** | Magnetic Resonance Spectroscopy |
| **ROS** | Reactive oxygen species |
| **α-SMA** | α-smooth muscle actin |

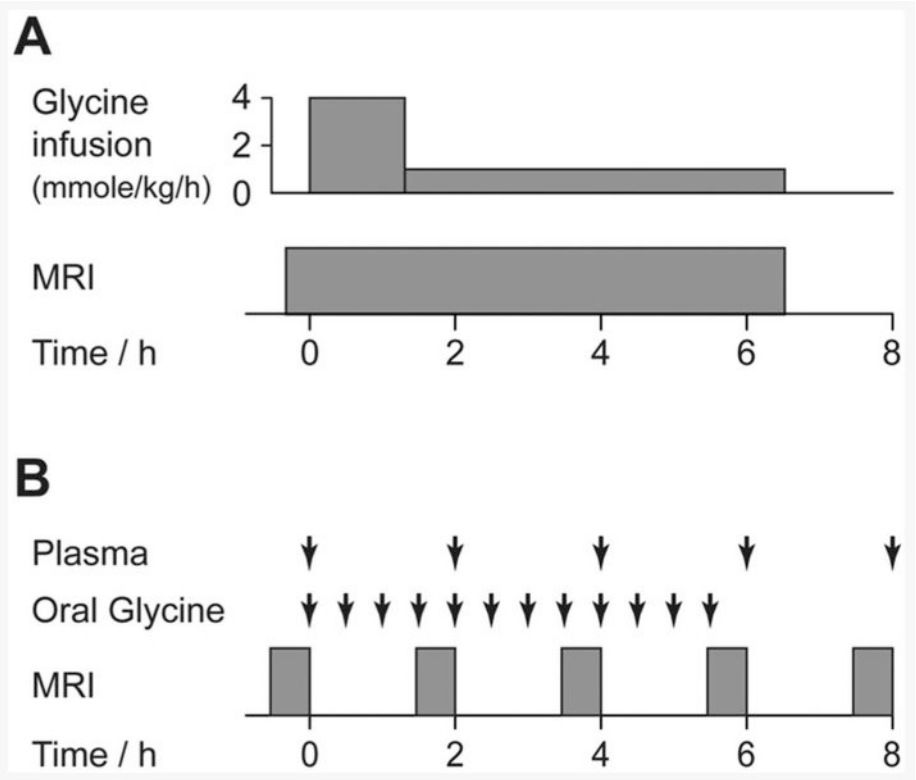


**Figure 1.**

MR study protocol summary. A: Preclinical study protocol showing timings of glycine infusion and MRI scanning. B: Human study protocol showing timings of blood sampling, oral glycine administration and MRI scanning.

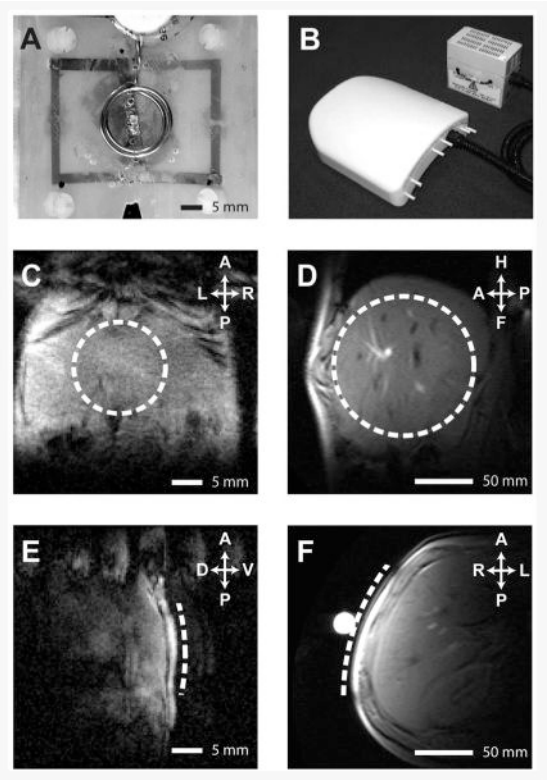


**Figure 2.**

$^{13}C/^{1}H$ RF coils, and MR images showing coil positioning. A&B: $^{13}C/^{1}H$ RF coils employed for preclinical and human studies respectively. C-F: Representative hepatic $^{1}H$ images showing location of $^{13}C$ surface coils (dashed line) for preclinical (C&E) and human (D&F) studies.

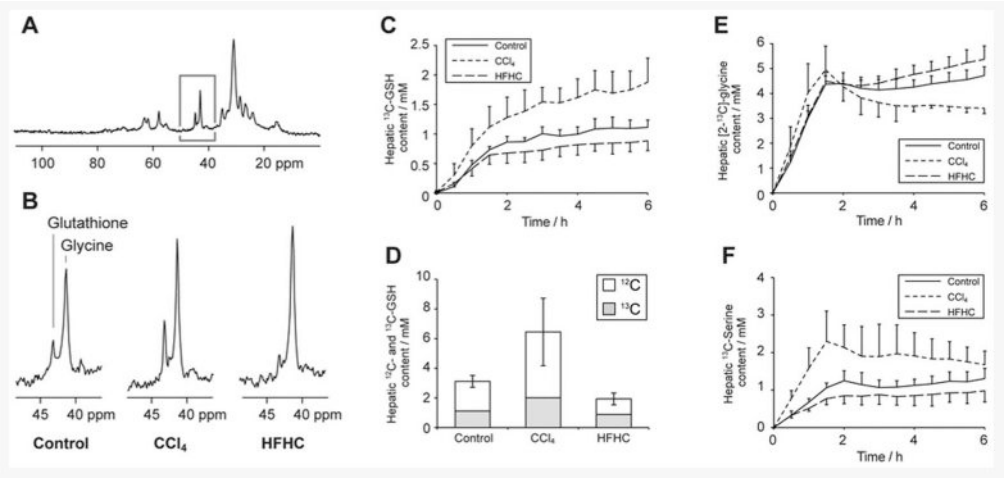


**Figure 3.**

Preclinical study $^{13}C$ MR data. A: Representative hepatic $^{13}C$ spectrum acquired after 6h of [2-$^{13}C$]-glycine infusion. B: Regions of the $^{13}C$ spectrum showing resonances from [2-$^{13}C$]-glycine and $^{13}C$-labelled glutathione from rats in each of the three study groups. C: Timecourse of hepatic $^{13}C$-labelled glutathione concentration in the experimental groups. D: Mean concentrations of $^{13}C$-labelled and total glutathione in the experimental groups at the end of the 6.5h experiment. E & F: Timecourses of hepatic [2-$^{13}C$]-glycine and [2-$^{13}C$]-serine concentration in the experimental groups.

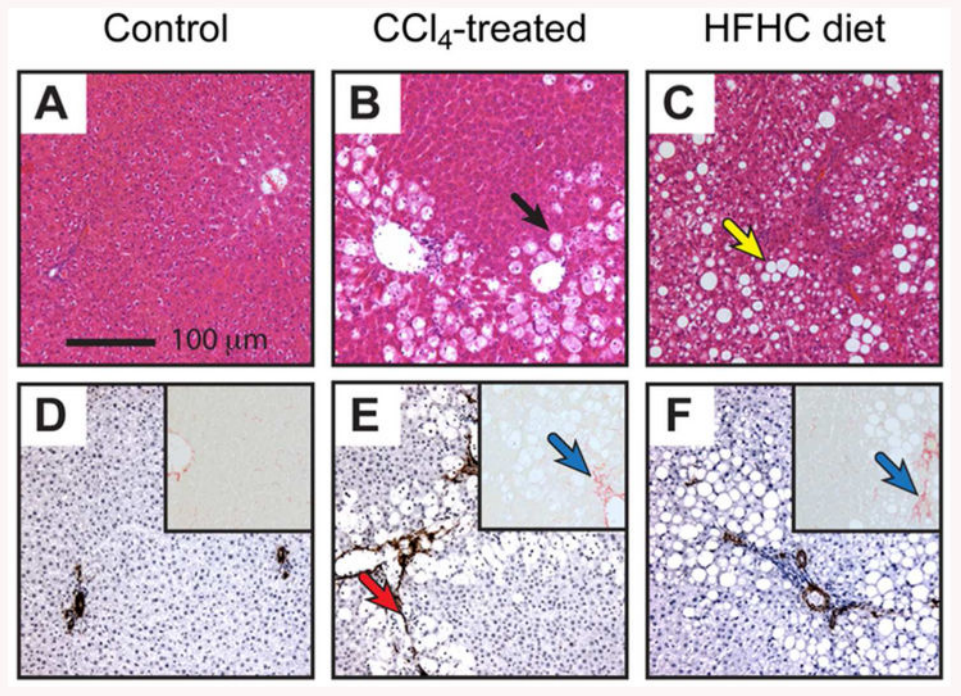


**Figure 4.**

Histological sections of rat liver from the preclinical study groups. A-C: H&E stained sections. D-F: α-SMA stained sections and Sirius Red stained sections (inset). Representative photomicrographs at x100 magnification of a minimum of n=3 rats per group. Black arrow indicates damaged hepatocytes, yellow arrow indicates fat deposition, red arrow indicates α-SMA staining of myofibroblasts, blue arrows indicate collagen deposition.

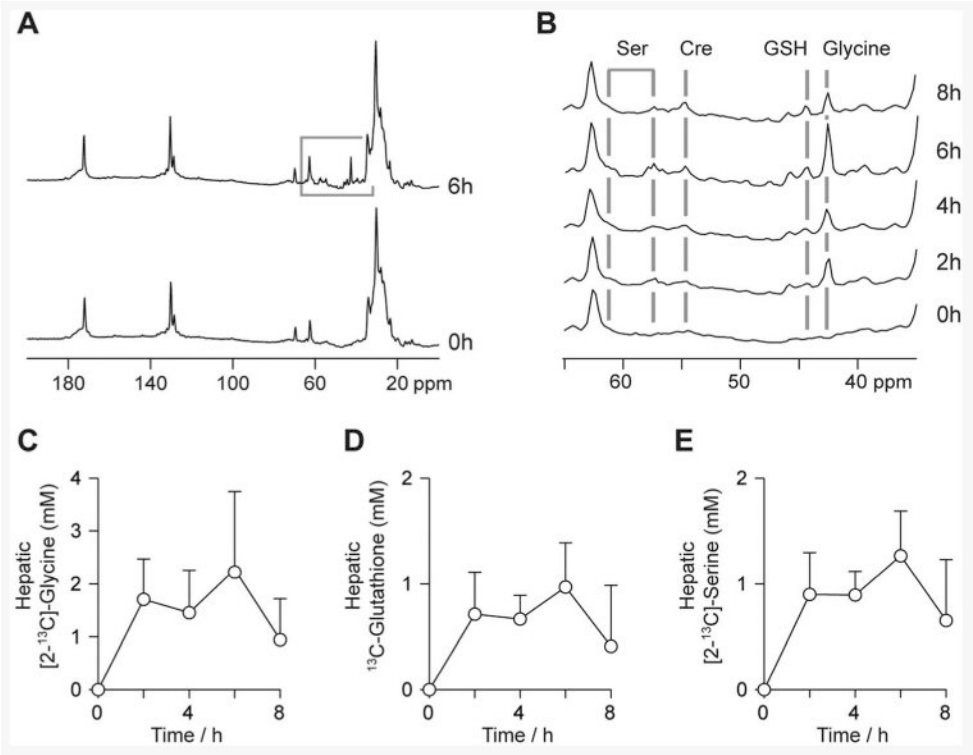


**Figure 5.**

Human study $^{13}C$ MR data. A: Hepatic $^{13}C$ spectra from a study volunteer prior to and after the 6h glycine ingestion period. B: Region of the $^{13}C$ spectrum from a study volunteer showing resonances from [2-$^{13}C$]-glycine, and endogenously $^{13}C$-labelled glutathione, serine and creatine. C-E: Mean concentrations of [2-$^{13}C$]-glycine, $^{13}C$-labelled glutathione and [2-$^{13}C$]-serine over the experimental timecourse.

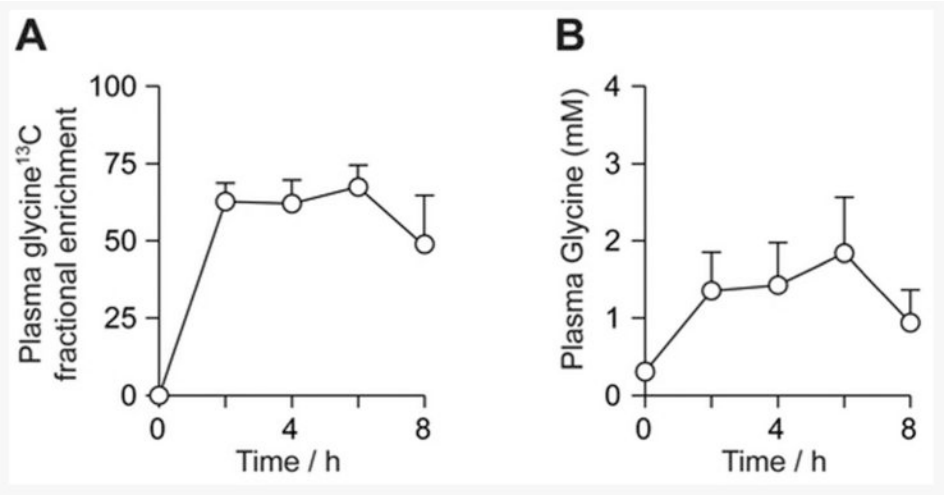


**Figure 6.**

Human study plasma glycine analysis. A: Mean $^{13}C$ fractional enrichment of plasma glycine. B: Mean glycine (unlabelled + labelled) concentration over the experimental timecourse.

**Table 1**

Preclinical study morphometric measurements, plasma biochemical analysis, and hepatic isoprostane content analysis.

| | Body mass (g) | Liver mass (g) | ALT (U/L) | AST (U/L) | Alk phos (U/L) | Hepatic isoprostane content (ng/g) | | |
|---|---|---|---|---|---|---|---|---|
| | | | | | | $F_2$-III | $F_2$-IV | $F_2$-VI |
| Control | 220 ± 33 | 10.8 ± 0.8 | 49 ± 8 | 71 ± 6 | 290 ± 17 | 1.4 ± 0.3 | 0.06 ± 0.19 | 1.7 ± 0.2 |
| $CCl_4$ | 243 ± 27 | 11.6 ± 0.8 | 378 ± 84 | 950 ± 378 | 281 ± 27 | 46.7 ± 10.9 | 0.90 ± 0.19 | 36.4 ± 3.2 |
| HFHC diet | 527 ± 67 | 17.0 ± 3.1 | 74 ± 34 | 200 ± 140 | 136 ± 43 | 20.2 ± 2.8 | 0.60 ± 0.14 | 5.7 ± 1.3 |